



A Numerical study of Two-Phase flow through a Rectangular Duct with a Convergence Rib

Riyadh.S.Al-Turaihi^{*1}, Abbas Sahi Shareef², Ali Abdalaimma³

¹University of Babylon, ^{2,3}University of Kerbela

^{*}Corresponding Author E-mail: riyadhalturaihi@gmail.com

Abstract

Two-phase flow in ribbed convergent rectangular upward vertical duct was studied. Water and air were used as materials for two-phase. Numerical studies have been performed to test the influence of increased air and water discharges on the pressure profile and pressure drop through the convergent section, as the effect of increasing the convergent angle on the pressure difference across the convergent section was studied.

Water inlet discharges used were between (5-20 L/min), and air discharges were between (5.833-16.666 L/min). Two test channels with convergent angles (10 and 15 degrees) were used.

Computational fluid dynamics for a three-dimensional model was simulated with ANSYS fluent 18 depending on the boundary condition and governed by equations of Eulerian multiphase flow model.

The results indicated that the pressure along the test channel raises as water and air discharge rise. It was observed too the pressure drop increases with the increase of the convergence angle.

Keywords: Simulation of two-phase flow, Convergence ribs rectangular duct, Convergence angle, pressure drop.

1. Introduction

Two-phase flow is defined as two-phase flow simultaneously in the same pipe like gas and liquid, gas and solid, two dissimilar liquids or liquid and solid. The most complexes of these types is the flow of gas-liquids due to the compressibility and deformation of both phases. Two-phase flow can be often met in chemical or mechanical engineering applications, oil wells, power generation, reactors, boilers, condensers, evaporators and combustion systems [1]. The existence of geometrical singularities in pipes may significantly impact the behavior of two-phase flow and thus the resulting pressure drop. Therefore, it is a significant issue of study in specific when the application concerns industrial safety valves. The studies of two-phase flow in straight channels are numerous in the survey review. In contrast to the studies of two-phase flow in divergence, convergence, bends and other types of singularities are somewhat few. The purpose of studying these geometries is to find how these geometrical accidents affect the two-phase flow regimes and pressure distribution. Especially, the understanding of the flow in such basic geometries can lead to an improved design of safety systems [2]. Behzadi et al [3] improved the Eulerian approach for two-phase flow (bubble flow) with a high void fraction. A bubble flow simulator was also performed successfully through a sudden divergent section. Cheng [4] conducted a comprehensive review of previous studies which deals with two-phase flow (gas-liquid) flow patterns and flow maps for adiabatic and non-adiabatic conditions. It was noted that the Conclusions, which obtained from different researchers were not corresponding under the same test conditions

and same fluids. Because Most researchers used classical visual-only method In their studies of flow patterns. Zhu [5] Conducted a numerical study of the effect of hydrofoil on the distribution of bubbles for the bubble flow of different ranges of attack angles and Reynolds number. It was observed that the effect of the attack angle was small at Reynolds number low, but the effect increased with the increase in Reynolds number. It was also observed that the angle of attack on the distribution of the bubble was clearer at the angle of 20 instead of 10 degree. Roul and Dash [6] employed the Eulerian-Eulerian approach with turbulent model k-epsilon; the results show the numerical values for pressure difference across sudden enlargement was good agreement with experimental values. It was also concluded that the mixture model is better than the homogeneous model to obtain an acceptable numerical simulation. Sakr et al [7] used SST (K- ω) turbulent model for a numerical simulation. It was found that this model gives accurate results for two-phase flow across the sudden enlargement. Eskin and Deniz [8] The Eulerian approach was used with RMS turbulent model for two-phase flow through sudden enlargement. It was observed that the deviation between the numerical values of void fraction and the pressure difference with the experimental values was increased with the increase of the void fraction. Ueda et al [9] used The volume of fluid VOF model, which includes the effect of wall adhesion and surface tension on flow, it was successfully predicted for the bubble flow pattern for low gas discharge and annular flow pattern for high gas discharge. Kumer [10] Performed numerically simulation for water oil two-phase stratified flow in the horizontal and inclined pipes by using volume of fraction (VOF) approach and RNG k- ϵ

turbulence model. The angle of inclination had been ranged from ± 50 , 00 , ± 100 from the horizontal. Selected models were successfully predicted the flow pattern, local phase fraction, slip ratio, pressure drop, turbulent kinetic energy, and turbulent energy dissipation rate. Ahmadpour et al [11] conducted a numerical simulation for the two-phase flow (water-air) through divergence/convergence of constant opening angles; the $k-\epsilon$ turbulence model was used. The results obtained were compared with previous surveys. The effect of void fraction, opening angle and Reynolds number was studied on pressure distribution inside a test channel this work, an experimental and numerical study of two-phase flow was carried out across a gradual divergent section. The effect of increasing the discharge of air and water and increasing the angle of divergent to recovery pressure through this section. The objectives for the present work investigate the effect of water discharge, air discharge and a convergence angle on the pressure profile and drop pressure across vertical ribbed convergence section. As compared of experimental and numerical results obtained from the program of ANSYS.

2. Numerical Work

For the numerical simulation, the computational fluid dynamics (CFD) software has been applied for modeling water-air flow through a vertical convergence rectangular duct contains ribs, Euler multiphase- VOF model was used with the Renormalization Group $k-\epsilon$ turbulent model. The analysis and construction of the numerical field are performed in fluent (ANSYS18.0) CFD.

2.1. Geometry Model

A SolidWorks 2013 was used to draw the geometry of the system as a three-dimensional structure for a numerical simulation of gas-liquid flow through a convergence section. The geometry was drawn with dimensions 2×8 cm before the convergence section, the length was 0.5 m long, while the section area was 2×6 cm after the convergence section with a length of 0.15 m. The convergence section has four ribs, two ribs on each side with dimensions $0.5 \times 0.5 \times 2$ cm as shown in Figure 1a, b for convergence angle 10, 15 degree, respectively. A circle with diameter 0.00126 m was drawn inside a rectangle in the bottom surface of the structure. So that circle represents entry of air into the test channel and the remaining area represents the entry of water, as shown in Figure 2. All sides of the structure were set to be adiabatic walls. The bottom surface of the duct was set to represent the entry of air and water into the test channel, while the top surface of the duct was set to represent the outlet flow.



Fig. 1a: The geometry with $\theta = 10$ degree



Fig. 1b.: The geometry with $\theta = 10$ degree

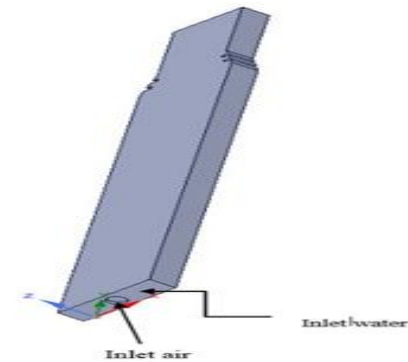


Fig. 2: Inlet of air and water

2.2. The Mesh

Meshing is an important part of the numerical simulation process. The mesh influences the accuracy, convergence, and speed of the solution [12]. The smaller elements are given more accurate results with taking into account computational cost. In this work, meshing was performed by using the ANSYS Workbench 18.0, where the geometry was divided into small square elements with a size of 0.001 cm for maximum and minimum, because the results are fixed at these values of mesh size (number of nodes and elements is 1080912 and 1013420 respectively for test section with convergence angle 10 degree and number of nodes and elements is 1042902 and 977600 respectively for test section with convergence angle 15 degrees), as shown in figure 3. Figures 4a,b show the mesh of the two-phase flow in the convergence section with 10 and 15 degrees, respectively.

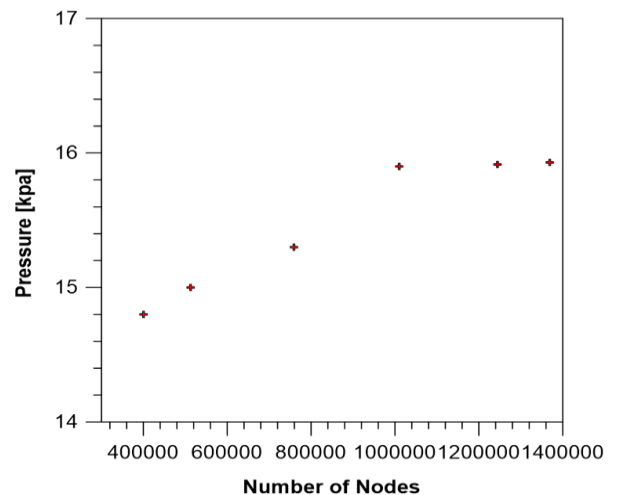


Fig. 3: Test of number size of mesh

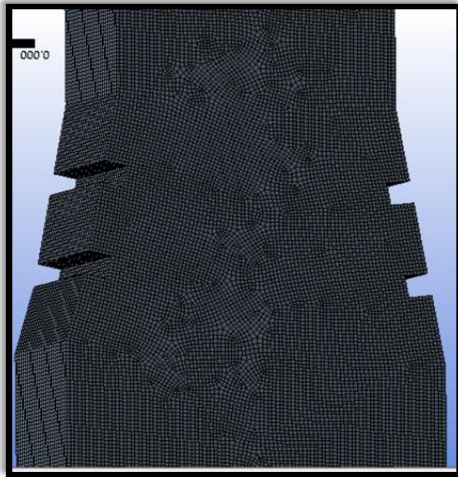


Fig. 4 a: The mesh of convergence with $\theta = 10$ degree

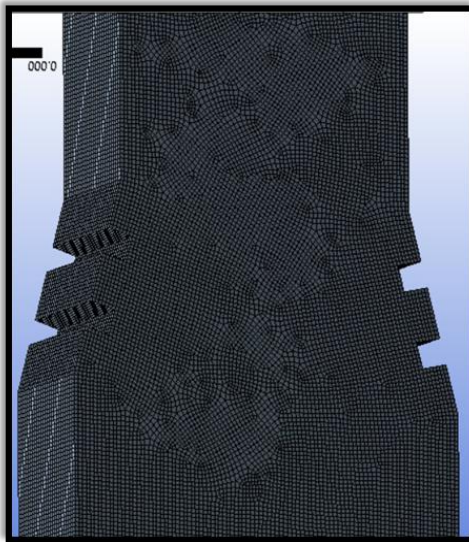


Fig. 4b: The mesh of convergence with $\theta = 15$ degree

2.3. Governing Equations

A volume of Fluid model solves the volume fraction equation and conservation equations of momentum for each phase. This model is more suitable and accurate for present work. A volume of Fluid model is defined as the integration of properties of fluids in the control volume, namely the volume of a computational mesh element. The volume fraction of every fluid is tracked through every element in the computational mesh, while all fluids share a one set of momentum equations. When an element is empty with no traced fluid inside, the value of α_q is zero; when the element is complete, $\alpha_q = 1$; and when there is a fluid interface in the element, $0 < \alpha_q < 1$. The domain is modeled as 3-D, according to boundary conditions of mixture internal flow and by pressure-based solver calculated a solution. The momentum equation is solved by depending on variables such as phases volume fractions, and properties: density (ρ), and viscosity (μ) [12].

2.3.1. The Volume Fraction Equation

The evolution of the q-the fluid in a system on (n) fluids is governed by the transport equation.

$$\frac{\partial \alpha_q}{\partial t} + \vec{v} \cdot \nabla \alpha_q = \frac{S_{\alpha_q}}{\rho_q} \quad (1)$$

With the following constraint

$$\sum_{q=1}^n \alpha_q = 1 \quad (2)$$

By default, the source term on the right-hand side of Equation (1) is zero, but you can identify a constant or user-defined mass source for each phase.

For every element, The Characteristics of mixture like dynamic viscosity and mixture density are based on the volume fraction of all phases as given by Eq:

$$\rho = \sum \alpha_n \rho_n ; \mu = \frac{\sum \alpha_n \rho_n \mu_n}{\sum \alpha_n \rho_n} \quad (3)$$

2.3.2. The Momentum Equation

One momentum equation is resolved during the field, and the resulting velocity field is shared among the phases. The momentum equation, shown below, is based on the volume fractions of all phases through the characteristics of ρ and μ .

$$\rho \frac{\partial}{\partial t} (\rho \vec{v}) + \nabla \cdot (\rho \vec{v} \vec{v}) = -\nabla p + \nabla \cdot [\mu (\nabla \vec{v} + \nabla \vec{v}^T)] + \vec{g} + \vec{F} \quad (4)$$

Where \vec{v} is velocity field and \vec{F} is a body force.

2.3.3. Turbulence Model

ANSYS Fluent 18.0 presents three approaches for the k-epsilon turbulence model in the multiphase flow

1. Turbulence mixture model
2. Turbulence dispersed model
3. Turbulence model for each phase

Turbulence Re-Normalization Group mixture model was set for the two-phase flow model because this model is used for swirl flow, noting that the difference is closed in the case of comparing the results obtained from the use of this model with the standard k-epsilon model, which can be defined through these equations [12].

$$\frac{\partial}{\partial t} (\rho_m K) + \nabla \cdot (\rho_m \vec{V}_m K) = \nabla \cdot \left(\frac{\mu_{t,m}}{\sigma K} \nabla K \right) + G_{K,m} - \rho_m \epsilon \quad (5)$$

$$\frac{\partial}{\partial t} (\rho_m \epsilon) + \nabla \cdot (\rho_m \vec{V}_m \epsilon) = \nabla \cdot \left(\frac{\mu_{t,m}}{\sigma \epsilon} \nabla \epsilon \right) + \frac{\epsilon}{K} (C_{1\epsilon} G_{K,m} - C_{2\epsilon} \rho_m \epsilon) \quad (6)$$

Where k is turbulent kinetic energy, ϵ is the turbulent dissipation rate, G is the energy, σ and is the turbulent Prandtl number for K and ϵ .

The density and the velocity of the mixture can be found by using Eqs. (7) and (8), respectively.

$$\rho_m = \sum_{i=1}^N \alpha_i \rho_i \quad (7)$$

$$\vec{V}_m = \frac{\sum_{i=1}^N \alpha_i \rho_i \vec{V}_i}{\sum_{i=1}^N \alpha_i \rho_i} \quad (8)$$

The turbulent viscosity and kinetic energy of the mixture can be found by using Eqs. (9) and (10), respectively.

$$\mu_{t,m} = \rho_m C_m \frac{K^2}{\epsilon} \quad (9)$$

$$G_{K,m} = \mu_{t,m} \left(\nabla \vec{V}_m + (\nabla \vec{V}_m)^T \right) : \vec{V}_m \quad (10)$$

The model constants can be seen in Table 1

Table 1. Model Constants

The constant	Value
C_m	0.09
$C_1 - \text{Epsilon}$	1.44
$C_2 - \text{Epsilon}$	1.92
σ_k	1
σ_ϵ	1.3

2.4. Convergent Criteria

Every numerical basis solution contains errors. The key is to know how those errors are big and whether the numerical results are acceptable in the engineering applications. In the present numerical Convergence was accepted as being completed when the residual curve reached 10^{-4} . Table 2 shows the residual error.

Table 2. Residual error for the tested case

Equation s	Continuity	X- Velocity	Y- Velocity	energy	k	E	Volume Fraction
Residual Error	10^{-5}	10^{-4}	10^{-4}	10^{-6}	10^{-4}	10^{-4}	10^{-4}

3. Program Validation

For verifying the numerical code, the calculated axial profile of pressure is compared with numerical results previously studied. By Ahmedpour 2016 [11] for two-phase flow (water and air) through graduationsmooth divergence circular vertical channel. The case was for $Re_L = 1.8 \times 10^5$, $\beta = 20\%$, $\sigma = 0.43$ and different opening divergence angle of 15 degrees as shown in Figure 5. A good agreement is detected between the numerical results of pressure and numerical results of Ahmedpour [11] with average percentage error was (9.11) %. Which validates the accuracy of the numerical code.

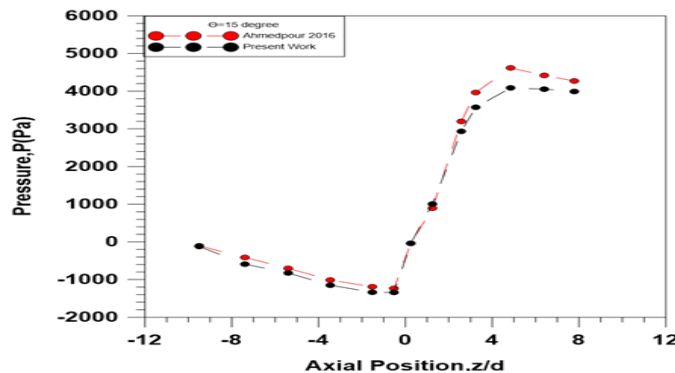
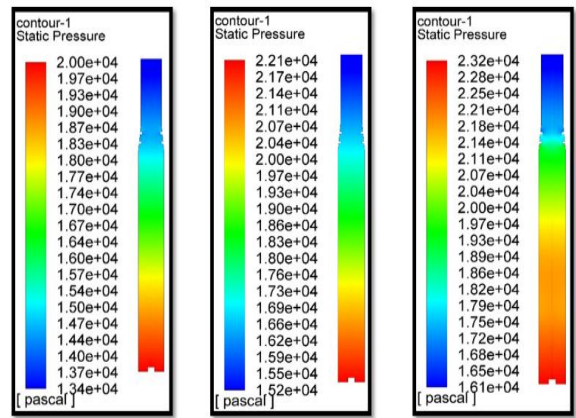


Fig. 5: The validation of numerical code with numerical results of Ahmedpour

4. Results and Discussion

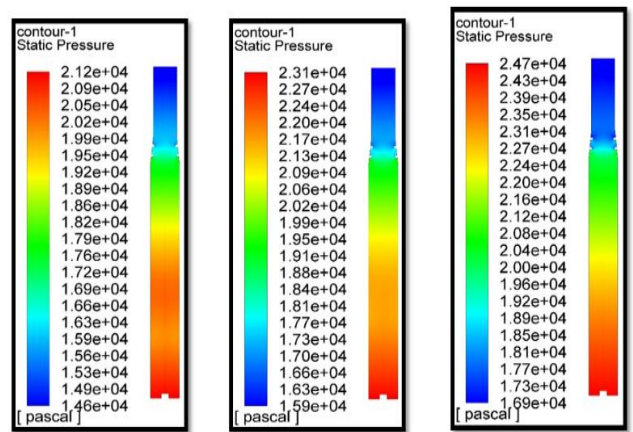
4.1. Effect of water and air discharge on the pressure profile

The numerical results of the impact of increasing air and water discharge on the pressure profile can be shown in figures 6 to figure 8. It can be seen from these figures that the pressure of the test channel decreased from the bottom to the top, especially in the convergence section. Can be seen too that pressure profile increases with increased air or water.



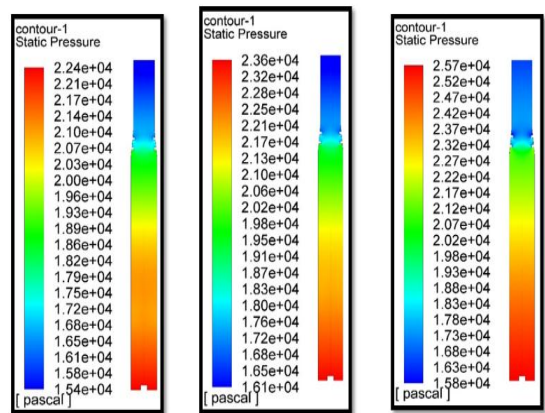
(a) Q air =5.833 l/min (b) Q air =10.833 l/min (c) Q air =16.666 l/min

Fig. 6: The contour of pressure at Q water =5 L/ min, $\theta = 10$ degree



(a) Q air =5.833 l/min (b) Q air =10.833 l/min (c) Q air =16.666 l/min

Fig. 7: The contour of pressure at Q water =15 L/ min, $\theta = 10$ degree



(a) Q air =5.833 l/min (b) Q air =10.833 l/min (c) Q air =16.666 l/min

Fig. 8: The contour of pressure at Q water =20 L/ min, $\theta = 10$ degree

4.2 Effect of water and air discharge and convergence angle on pressuredrop

The numerical results of the effect of increasing air and water discharge and effect of increasing of opening angle on the pressuredrop through the convergence section can be shown in Figure 9 and 10. It can be seen from these figures that the drop

pressure increases with increasing discharge of air or water for both the 10 and 15 opening angles. It was observed, too, that pressure drop for the opening angle 15 is more than the drop pressure at the opening angle 10 at the same air and water discharge because the eddies are more for the case of angle 15 because of the additional flow area contributes to the promotion of pressure drop, leading to make the drop pressure more than the case of opening angle of 10 degrees.

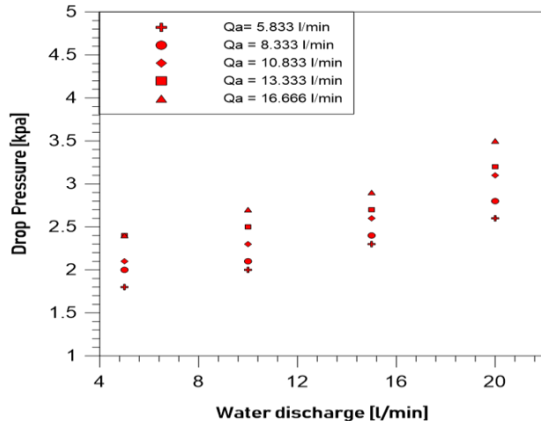


Fig. 9: Drop pressure for different values of water discharge at $\theta=15$ degree

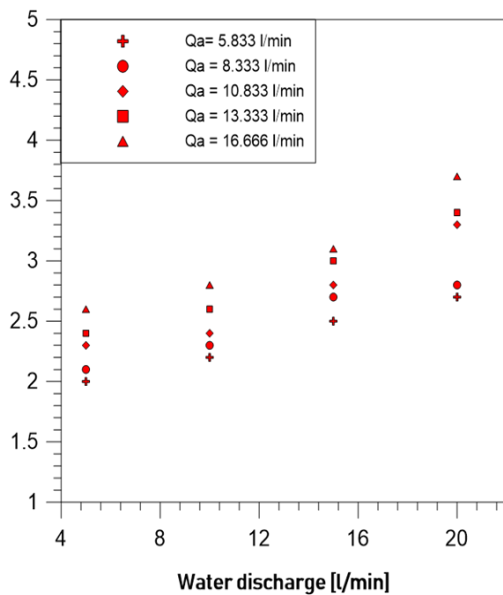
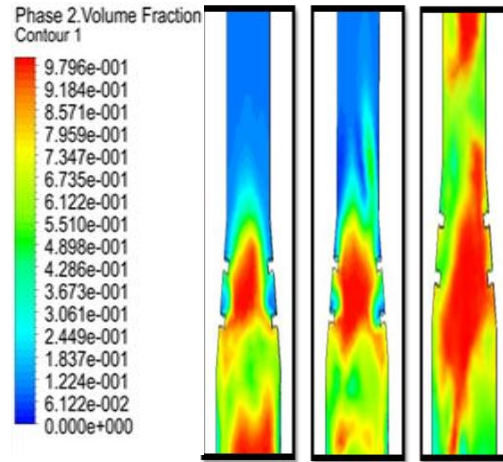


Fig. 10: Drop pressure for different values of water discharge at $\theta=10$ degree

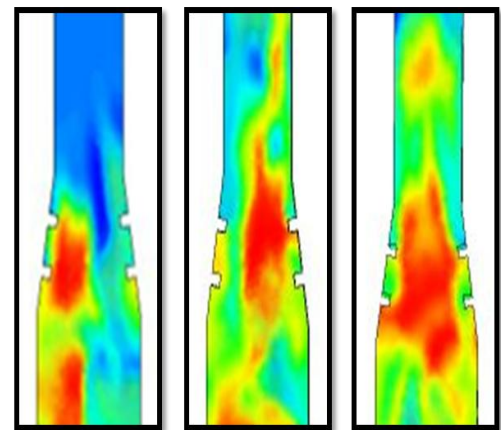
4.3 The influence of water and air discharge on the flow behavior

Figure 11 represents the numerical images for the two-phase flow behavior in the convergence ribs rectangular vertical duct for water discharge ($Q_w=5$ L/min) and air discharges ($Q_a=5.833$, 10.833 and 16.666 L/min), for the convergence angle 10 degrees. The figure 11a at $Q_a=5.833$ shows that the volume of the bubble is small due to the air and water discharges being low. Also, with the increase in air discharge, the volume of bubbles increases, as at $Q_a=10.833$ and $Q_a=16.666$ L/min as shown in figure 11b and 11c, respectively. With the continuing increase of water discharge, the volume of bubble decreases and the turbulence in flow and velocity of the vortex in the convergence section is higher compared with low air discharge cases as shown in figures 12 and 13.



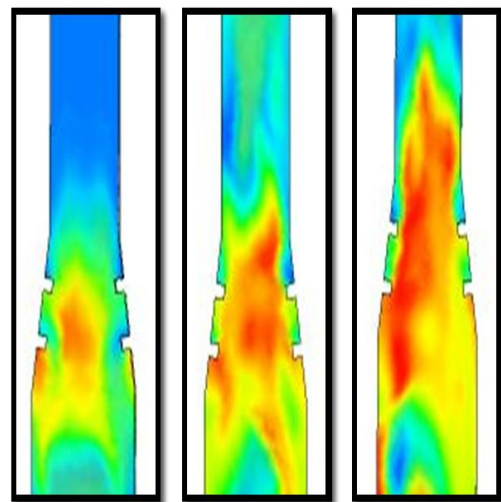
Q air (a) 5.833 (b) 10.833 (c) 16.666

Fig. 11: Void air fraction at Q water =5 L/min, $\theta = 10$



Q air (a) 5.833 (b) 10.833 (c) 16.666

Fig. 12: Void air fraction at Q water =15 L/min, $\theta = 10$



Q air (a) 5.833 (b) 10.833 (c) 16.666

Fig. 13: Void air fraction at Q water =20 L/min, $\theta = 10$

The figures 14a,b showed the velocity vector, note that the generated vortexes are affected by the increased discharge of air and water which leads to increased turbulence, also notice that the ribs have a role in changing the direction of velocity and thus generate further turbulence.

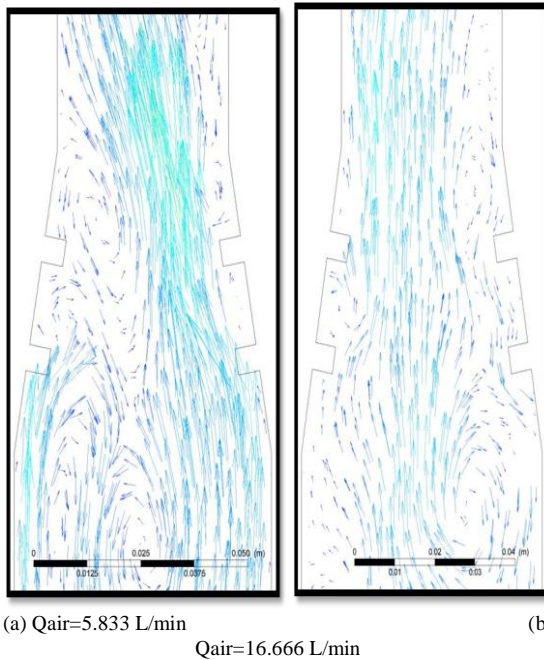


Fig. 14: Velocity vector at 5 L/min water discharge with $\theta=10$ degree

5. Conclusion

- 1- When water or air discharge increases, the pressure drop rises.
- 2-When the convergence angle increases, the pressure drop decreases because the eddies are more for the case of angle 15 because of the additional flow area contributes to the promotion of pressure drop, leading to making the drop pressure more than the case of the convergence angle of 10 degrees.
- 3-When air discharge increases, the volume and amount of bubbles increases. In addition, as continuous air discharge increases, flow turbulence increases as does the velocity of generating eddies.
- 4-The volume of bubbles decreases when water discharge increases. Also, as continuous water discharge increases, the flow is more turbulent and unstable and eddies are stronger.
- 5-The effect of increases of water discharge on the turbulence is higher than the effect of increases of air discharge because the water density is higher and, thus, the inertia force is greater for the case of water.

Nomenclature

S Source term, dimensionless
 P Pressure, kpa
 g Acceleration gravity, m/s^2

Greek Symbols

θ Convergence angle
 α Volume fraction
 ρ Density, kg/m^3
 μ Dynamic viscosity, kg/ms
 K Turbulence kinetic energy, m^2/s^2
 ϵ Turbulence kinetic energy dissipation rate, m^2/s^2

Subscripts

n Number of phase
 q Phase
 m Mixture

Reference

- [1] A. J. Ghajar, "Non-boiling heat transfer in gas-liquid flow in pipes: a tutorial," *J. Brazilian Soc. Mech. Sci. Eng.*, vol. 27, pp. 46–73, 2005.
- [2] V. G. Kourakos, P. Rambaud, S. Chabane, D. Pierrat, and J. M. Buchlin, "Two-phase flow modeling within expansion and contraction singularities," vol. 63, pp. 27–43, 2009.
- [3] A. Behzadi, R. I. Issa, and H. Rusche, "Modelling of dispersed bubble and droplet flow at high phase fractions," *Chem. Eng. Sci.*, vol. 59, pp. 759–770, 2004.
- [4] L. Cheng, G. Ribatski, and J. R. Thome, "Two-Phase Flow Patterns and Flow-Pattern Maps: Fundamentals and Applications," *Appl. Mech. Rev.*, vol. 61, pp. 50802, 2008.
- [5] S. Zhu, H. Blackburn, and B. Anderson, "Numerical simulations of bubble dispersion over a hydrofoil," *7th Int. Conf. CFD Miner. Process Ind.*, pp. 1–6, 2009.
- [6] Roul, M. K., Dash, S. K., "Two-phase pressure drop caused by sudden flow area contraction/expansion in small circular pipes," *Int. J. Num. Methods Fluids*. vol. 66, pp.1420-1446, 2011.
- [7] I. M. Sakr, A. Balabel, K. Ibrahim, and S. El-kom, "Computations of Upward Water / Air Fluid Flow in," vol. 4, , pp. 193–213, 2013.
- [8] N. Eskin and E. Deniz, "Pressure Drop of Two-Phase Flow through Horizontal Channel with Smooth Expansion," *Int. Refridgeration Air-Conditioning Conf.*, pp. 1–10, 2012.
- [9] Ueda, Y., Nakajima, T., Ishii, T., Tsujino, R., Iguchi, M., "Numerical simulation of gas liquid two- phase flow in a horizontally placed hydrophobic rectangular channel", *High Temperature Material Proc.*, vol.31, pp.405-410, 2012.
- [10] V. Kumar, "NUMERICAL STUDY OF OIL-WATER TWO PHASE FLOW IN HORIZONTAL & INCLINED TUBES," 2014.
- [11] A. Ahmadpour, S. M. A. Noori Rahim Abadi, and R. Kouhikamali, "Numerical simulation of two-phase gas-liquid flow through gradual expansions/contractions," *Int. J. Multiph. Flow*, vol. 79, pp. 31–49, 2016.
- [12] Fluent User's Guide (2006). Modeling Multiphase Flow, Fluent Inc.